PARAMETRIC ANALYSIS OF AERODYNAMIC CHARACTERISTICS OF LAUNCH VEHICLES WITH STRAP-ON BOOSTERS

Arash Naghib-Lahouti[1], Amir Nejat[2], Taravat Khadivi[3]
1- Faculty Member 2,3-Senior Research Engineers
Aerospace Research Institute, *PO Box 15875-3885,Tehran, Iran*

Keywords: *launch vehicles, aerodynamic, strap-on boosters, parametric analysis*

Abstract

An engineering code has been developed for estimation of longitudinal aerodynamic coefficients of a multi-body launch vehicle with strap-on boosters, based on their geometric characteristics and flow conditions. The code, which incorporates data from empirical/analytical methods, CFD analysis, wind tunnel tests and similar engineering codes has been used for parametric analysis of the effects of angular position of strap-ons, the gap between the core and strap-ons, angle of attack, and Mach number on aerodynamic coefficients (C_N and C_A) of a generic geometry, defined by statistical investigation of actual launch vehicles. Results indicate suitable accuracy within the range of $0^\circ<\alpha<16^\circ$ and $M<5.0$ for the purpose of preliminary aerodynamic design.

1 Introduction

Launch vehicles are used for delivering payloads to a specified altitude at the proper orbital velocity. The usual values of orbital velocities are too high to be achieved with a single stage vehicle [1]. A considerable part of a launch vehicle's propellant is consumed during the early stages of acceleration after lift-off, making it unnecessary to carry the partially depleted tanks, which can be ejected after depletion. On the other hand, various levels of thrust might be required in different phases of flight. Because of these problems, efforts have been made to develop propulsion systems with variable thrust. A multi stage system is a trivial solution [2,3].

Parallel staging, which appears in many launch vehicles developed since 1970s, is one of the most frequently used configurations. In this type of staging configuration, 2 to 9 solid or liquid propellant boosters join the first stage as strap-ons. They are usually ignited simultaneously together with the core engine(s) to provide the maximum thrust, and are separated from the core upon burn-out, to reduce the total weight of the climbing vehicle.

Despite their positive contribution to the performance of the vehicle, they bring about some difficulties to the design process. The strap-on boosters usually have large volumes and affect the external geometry considerably. The complex flow field around the multiple bodies, and the interference effects among them causes problems in the vehicle's aerodynamics. The vehicles experiences increased drag while the boosters are on, and safe separation of the boosters in an interference dominated flow field is also of great importance.

These issues show the necessity of aerodynamic analysis with various levels of accuracy throughout the design process. The estimated aerodynamic characteristics are particularly useful for structural/thermal analysis, trajectory and stability calculations, and the design and sizing of separation mechanisms.

The number of published articles in the field of multi body launch vehicle aerodynamics is unexpectedly low. A few selected studies are reviewed herein.

Reference [3], describes the studies on launch vehicle aerodynamics at Vikram space

center of India. Flow around various geometries of launch vehicles are modeled using panel method, to study the effects of geometric parameters such as number of strap-ons, the ratio of strap-on radius to core stage radius, and the gap between the core and strap-ons on the vehicle's aerodynamic characteristics.

Reference [4] deals with numerical simulation of inviscid supersonic flow around the multi body configuration using overlapping grid technique. Euler's equations have been integrated in their conservative form, and time marching method has been used for capturing shock waves. Flow pattern around the launch vehicle and shock reflections in the gap have been studied at zero angle of attack.

Reference [5] reports numerical solution of inviscid supersonic flows around a launch vehicle with 4 strap-on boosters. The overlapping grid technique has been used to simulate the flow at various angles of attack. Flow in the gap and the local subsonic flow in that region at a non-zero angle of attack have been addressed for the first time in this study. The effects of gap size and Mach number on the interference dominated flow field around the vehicle are investigated. A new method called NND has been employed for solving Euler's equations, and time marching has been used for capturing shock and expansion waves in the flow field.

An example of experimental investigation of the effects of strap-on boosters on aerodynamic characteristics of a launch vehicle is presented in reference [6]. In that study, the effects of adding strap-ons of various sizes on C_N, C_A and C_M in a range of supersonic Mach numbers have been evaluated.

In most references, the geometric model represents an actual launch vehicle in the early stages of its development, and few variations of configuration and geometry are dealt with. Flight conditions and velocity regimes are also limited to those occurring in each vehicle's actual or estimated flight profile.

2 Engineering codes for aerodynamic analysis and design of launch vehicles

Analytical methods, empirical techniques, CFD and wind tunnel testing are commonly used for aerodynamic analysis of a launch vehicle depending on the level of accuracy needed in different phases. Each of these tools has their own specific advantages and disadvantages.

In the conceptual design phase of a launch vehicle with strap-on boosters, a preliminary estimate of the vehicle's aerodynamic coefficients is needed, while the external shape and dimensions of each proposed configuration is yet to be defined and fixed. Several cycles of overall aerodynamic analysis might be necessary before selecting a final configuration and fixing the external geometry through a compromise with other aspects of the design process such as payload capabilities, propulsion and structural considerations.

Analytical methods are usually limited to simple geometries and simplified flow conditions. Therefore, they are difficult, if not impossible, to apply in such a problem. CFD codes require considerable computer resources and time for producing appropriate results, and are hardly economic for use as an intermediate tool in conceptual design cycles. Wind tunnel tests usually produce the most dependable results, but require a fixed external geometry, which can be far from being achieved in conceptual design. The costs associated with testing numerous proposed configurations are usually beyond limits of a conceptual design process [6,7].

As a result, an engineering code may be the only feasible tool for conceptual design. But it has to satisfy two important requirements. It must be able to handle the specific geometry and configuration of the vehicle, and its database, which normally integrates analytical and empirical techniques, must cover the intended flight conditions [8]. For example Missile Datcom, a well-known engineering code, covers a major part of the atmospheric flight regime of a launch vehicle, but is not able to handle a multi body configuration with strap-on boosters.

To overcome this shortcoming, an engineering code named AEROLAUNCH is being developed by the authors. This code, which is similar to Missile Datcom in structure, is able to produce longitudinal aerodynamic coefficients (C_N, C_A, C_M) for a launch vehicle with strap-on boosters in a range of flight conditions. Results of extensive CFD modeling and analysis of such geometries, and wind tunnel tests to verify the results, are incorporated in the code. With enrichment of the code's database through more CFD analysis and wind tunnel tests, its capabilities in terms of acceptable geometries and flight conditions are still being expanded.

3 Initial validation

To evaluate performance and accuracy of the code introduced in section 2, wind tunnel test results for a rocket with strap-on boosters [9] are compared with the code's results. The test geometry is shown in figure 5. The experiments have been conducted with two types of strap-ons, named "Large Booster" and "Small Booster".

The code's results for C_N in various Mach numbers and angles of attack have been compared with experimental results for both types of boosters. In most cases, the code's results display better agreement with experimental results when small boosters are on. This trend of agreement remains almost unchanged in all Mach numbers. The results for C_N at M=2.36 with different configurations are shown in figure 6 for comparison. It can be seen that the computational and experimental results follow the same trend when angle of attack varies, and the values are also in a relatively good agreement. The maximum difference between computational and experimental results is around 14% in the body+booster configuration and around 20% in the wing+body+booster configuration. Since sufficient information is not provided in reference [9] about calculation of base drag, a meaningful comparison between the code's results and the experimental results for axial force is not possible. However, even when the entire component of base drag is accounted for in the code, the results fall 25-50% short of experimental results.

4 Parametric analysis

Considering the promising results of the initial validation of AEROLAUNCH, a generic launch vehicle with strap-on boosters has been defined, and a systematic investigation of the effects of geometric and flow parameters on its aerodynamic characteristics has been conducted. These parameters include number of strap-ons, radius ratio, gap size, angular position of strap-ons around the core, Mach number and angle of attack. All calculations are carried out at standard sea level conditions, and the core's cross-section area is used as reference area.

4.1 Definition of the generic geometry

According to the information provided in reference [10], 29 families of launch vehicles exist. Taking different models in each family into account, we will have a total of 74 models of launch vehicles. 33 models (44% of the total) use strap-on boosters. In this section, it is intended to determine the dimensional data required for defining a generic geometry with strap-on boosters. The aim of defining this generic geometry is to investigate the effects of a number of parameters on its aerodynamic characteristics. Therefore, it is necessary to eliminate other parameters affecting the characteristics as much as possible.

The parameters selected for definition of the geometry are introduced in Figure 1, which displays the simplified geometry used for derivation of the parameters. A number of assumptions were made in order to simplify the geometry and the task of obtaining data for the parameters. These assumptions are presented graphically in Figures 2, 3 and 4.

Considering the assumptions, data for all launch vehicles except four, which have essential differences in shape with the generic configuration, have been derived. For some items of data, numerical values were not

provided in reference [10], and the values had to be determined by scaling the related drawings. 14 out of 33 models of launch vehicles with strap-on boosters have 4 boosters. 13 models have 2 boosters, 4 models have 6 boosters, 2 models have 9 boosters, and one has 3 boosters. (One model has two configurations: one with 2 and one with 4 boosters.)

The dimensional values are rounded before being used for aerodynamic analysis, in order to simplify data handling. The final selected dimensions of the generic geometry are presented in table 1.

Table 1- Parameters defining the simplified geometry

Parameter		Parameter	
L	50.0 m	L_S	21.0 m
L_N	4.5 m	L_{NS}	3.35 m
D	3.7 m	D_S	2.0 m
R	0.657 m	R_S	0.5 m
θ	17°	θ_S	14.5°

4.2 Effects of angular position of strap-on boosters

Angular position of strap-on boosters affects aerodynamic coefficients of the vehicle in non-zero angles of attack. To investigate these effects, two cases have been analyzed. These cases, named Phi0 and Phi1, represent two different ways of positioning strap-ons around the core (Figure 7). Obviously, as the number of strap-ons is increased, the difference between Phi0 and Phi1 cases reduces.

Figures 8 and 9 show variations of C_N vs. angle of attack in subsonic (M=0.6) and supersonic (M=3.0) regimes for body alone and body with 2 strap-ons in Phi0 and Phi1 cases. It can be seen that in Phi1 case, where strap-ons are in yaw plane, C_N is greater than that of Phi0 case. This can be explained by noting that in Phi0 case strap-ons are widely affected by the core's flow field in non-zero angles of attack. Their effective area for generation of normal force is therefore reduced.

Figures 10-13 show the same effect in Phi0 and Phi1 cases for the 4 and 6 strap-on configurations in M=0.6 and M=3.0, respectively. The figures indicate that the difference between Phi0 and Phi1 cases tends to reduce as the number of strap-ons is increased from 2 to 6. The angular position of strap-ons does not have any noticeable effect on C_A.

4.3 Effects of the gap between strap-ons and the core

In some launch vehicles, a gap exists between the core and strap-ons. The size of this gap affects aerodynamic interference between strap-ons and the core.

Figures 14 and 15 show C_N-Alpha curves for various gap sizes at M=0.6 for Phi0 and Phi1 cases. Figures 16 and 17 show the same results at M=3.0.

The figures indicate that an increase in gap size does not affect C_N in Phi0 case, but in Phi1 case an increase in gap size causes C_N to increase in each angle of attack.

Figures 18 and 19 show the effects of gap size on C_A in Phi0 case. The figures indicate that the effect of gap size on C_A is practically negligible. The results presented in this section are obtained by varying the gap size between 0 and 1m with 0.25m increments, for a 2 strap-on configuration in which each strap-on has a diameter of 2m.

4.4 Effects of strap-on radius

To investigate the effect of the radius of strap-ons, R_S (strap-on radius) is varied between 0.25m and 1m for a constant gap size of 0.5m. Figures 20-23 show variations of C_N-Alpha at M=0.6 and M=3.0 when the radius is changed in both Phi0 and Phi1 cases. It can be noticed that an increase in the radius ratio causes C_N to increase in constant angle of attack. This effect is more evident in Phi1 case. Variation of C_A-Alpha for different values of R_S is displayed in figures 24 and 25. C_A increases almost linearly as R_S is increased, but remains almost constant when angle of attack is changed within a limited range. The same behaviour has also been reported in reference [9].

4.5 Effects of the number of strap-ons

Effects of the number of strap-ons have been studied by analysing configurations with 0, 2, 4

and 6 strap-ons. As the number of strap-ons is increased, C_N increases at each constant angle of attack. The increase in C_N is greater in Phi1 case (Figures 26-29). As the number of strap-ons is increased, C_A increases almost linearly in a manner similar the one described in section 4.4. The curves presented in figures 30 and 31 are for Phi0 case. The curves for Phi1 case display the same behaviour and are not presented.

4.6 Effects of angle of attack

Except for those instances when the vehicle encounters wind gradients or performs transient manoeuvres, the angle of attack remains close to zero. In this study, a range of angles of attack from $\alpha=0^\circ$ to $\alpha=10^\circ$ is considered for investigation of the effects of flow direction on aerodynamic characteristics. In all of the curves presented in sections 4.2 through 4.5, the independent variable is angle of attack. As those curves indicate, the normal force coefficient C_N increases almost linearly when angle of attack increases in subsonic speeds. But in supersonic region, non-linear effects are evident in C_N-Alpha curves. The curves also indicate that C_A decreases slightly with an increase in angle of attack. This decrease can be explained considering variation of the direction of the free stream velocity vector. The major part of the change in the value of C_A is because of the core, since variation of C_A with angle of attack is almost negligible for strap-on boosters [9].

4.7 Effects of Mach number

A launch vehicle experiences all speed regimes, from subsonic to hypersonic, during its flight. But it faces different speed regimes in different configurations. For example, the vehicles that use strap-ons usually release them in supersonic speeds. Therefore, it is usually only the core that faces hypersonic speeds. The flight profile, which defines the vehicle's altitude, speed and position and occurrence of events such as stage separation in terms of the elapsed time, is different for every launch vehicle. Samples of actual flight profiles are presented in references [7] and [10].

All of the results presented so far in this study were for two Mach numbers only: M=0.6 as a representative of subsonic regime and M=3.0 as a representative of supersonic regime. However, to further evaluate the effects of Mach number, limited calculations have been performed in other Mach numbers for vehicles with 0,2 and 6 strap-ons in Phi0 configuration, at selected angles of attack of 0°, 4° and 8°. The results for C_N are plotted in figures 32-34 for a range of Mach numbers from 0.6 to 5.0. The sudden change of C_N at transonic Mach numbers, especially at higher angles of attack can be clearly noticed.

As Mach number is increased, C_N increases to reach its maximum at high transonic speeds. Afterwards, C_N decreases to reach a relative minimum at around M=4.

C_A behaves similarly as Mach number varies. In the transonic region, C_A shows a rapid rise because formation of weak shock waves begins. Figures 35 and 36 show variation of C_A with Mach number.

5 Conclusion

In this study, the role of different approaches to aerodynamic analysis of launch vehicles in different design phases was briefly described. A generic geometry was selected through statistical investigation of existing launch vehicles with strap-on boosters.

The generic geometry was modeled for analysis by an engineering code (AEROLAUNCH), to study the effects of such parameters as angular position of strap-ons around the core, radius and number of strap-ons, angle of attack and Mach number on the vehicle's normal and axial force coefficients (C_N and C_A).

Generally, the contribution of strap-ons to the vehicle's normal force reduces as they get closer to the pitch plane, because their exposed surface is reduced at non-zero angles of attack. Alternatively, when strap-ons are close to the yaw plane, their exposed surface is larger and this causes an increase in C_N.

The gap between the core and the strap-ons does not affect C_N and C_A when strap-ons

are positioned according to the configuration named Phi0. The same behavior is observed at all angles of attack having been studied. When the strap-ons are placed in the yaw plane (Phi1 case), C_N increases when the gap is increased, while C_A remains practically unaffected.

When the strap-ons' radius is increased (relative to the core stage), C_N and C_A increase. Naturally, the interference effects between the core and the strap-ons are also strengthened.

Increasing the number of strap-ons causes both C_N and C_A to increase proportionately in both Phi0 and Phi1 cases. Angular position of the added strap-ons affects the trend by which C_N increases.

As angle of attack increases, C_N increases while C_A decreases with a small slope.

In subsonic speeds, C_N and C_A increase due to compressibility effects when Mach number is increased. In transonic speeds, a rapid increase of C_A is observed, which is because of the drag rise due to formation of weak shock waves. C_N also increases considerably in this range. As Mach number increases further in the supersonic range, C_N and C_A decrease with a relatively small slope.

The promising results of the early validation of AEROLAUNCH, presented herein, encourage the authors to enrich the code's database and extend its capabilities to handle more complex geometries and flow condition by performing more CFD analysis and wind tunnel test on the selected geometries.

References

[1] Malina, F.J. and M. Summerfield. The problem of escape from the earth by rocket. *J. of Aeronautical Sciences*, V.14, pp. 476-478, Aug. 1947.

[2] Cornelisse, J.W. et al. *Rocket propulsion and space flight dynamics*. Pitman Pub., 1979.

[3] Devasia, K.J. et al. Investigation of inviscid flow field interference effects in strap-on configurations using panel method. *Proc. 13th Int. Symposium on Space Science and Technology*, Tokyo, Japan, June 1982.

[4] Singh, K.P. et al. Numerical simulation of inviscid supersonic flows over a launch vehicle with strap-on boosters. *AIAA Paper*, AIAA-87-0213-CP, 1987.

[5] Zhang Lumin, Yu Zechu and Yan Yongjian. Numerical simulation of inviscid supersonic flow over multiple bodies. *AIAA Paper*, AIAA-90-3099-CP, 1990.

[6] Mendenhall, M.R. et al. Aerodynamic design and analysis of a reusable launch vehicle. *Proc. ICAS 2000 Conference*, Harrogate, UK, Aug. 2000.

[7] Mendenhall, M.R. et al. Integrated aerodynamic design and analysis of launch vehicles. *AIAA Paper*, AIAA-2001-0263, 2001.

[8] Moore, F.G. et al. Evaluation and improvements to the Aeroprediction code based on recent test data. *Journal of Spacecraft and Rockets*, V.37, No.6, Nov.-Dec. 2000.

[9] Leroy-Spearman M. and R.H. Fournier. Effects of strap-on boosters on the aerodynamic characteristics of a simulated launch vehicle at Mach numbers from 1.50 to 2.86. *NASA Technical Memorandum* X-2491, Feb. 1972.

[10] Isakowitz, S.J. *The international reference guide to space launch systems*. 3rd Ed., AIAA, USA, 1999.

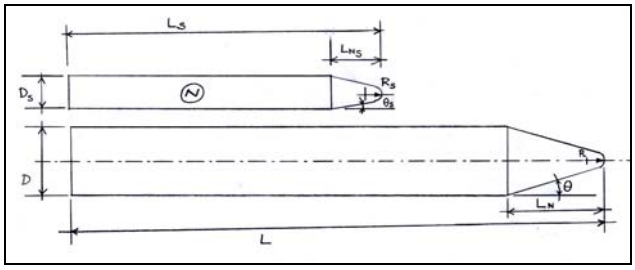

Figure 1- Simplified generic geometry

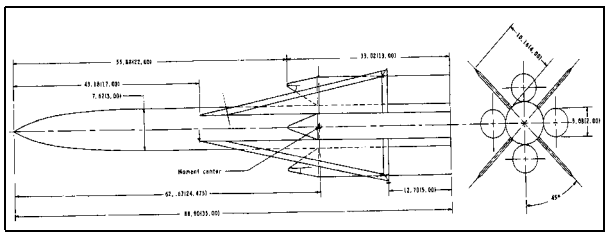

Figure 5- The vehicle with strap-on boosters (ref. [9])

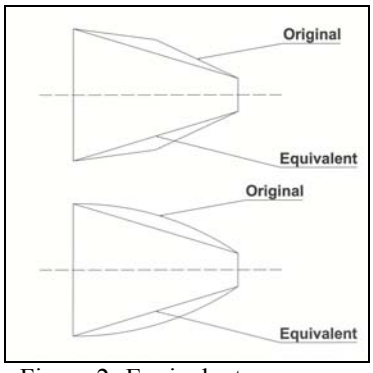

Figure 2- Equivalent nose cone

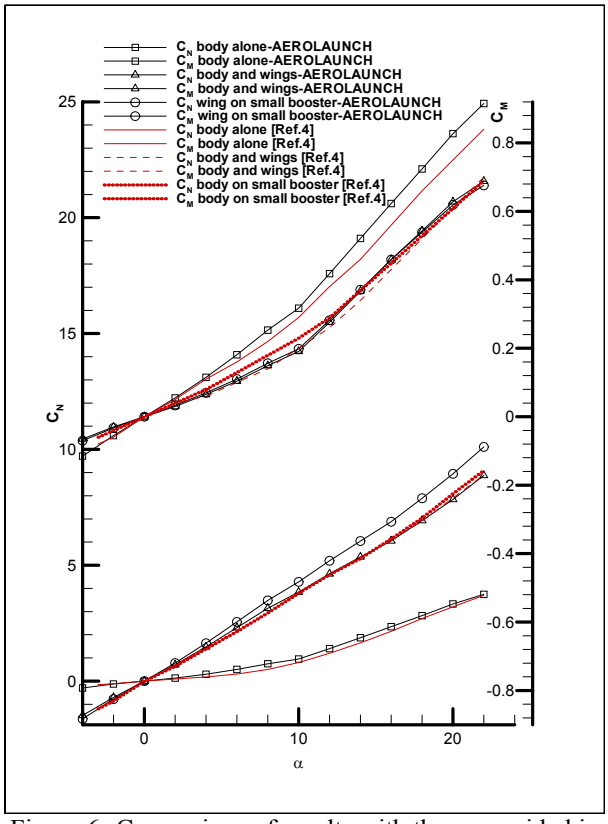

Figure 6- Comparison of results with those provided in ref. [9]

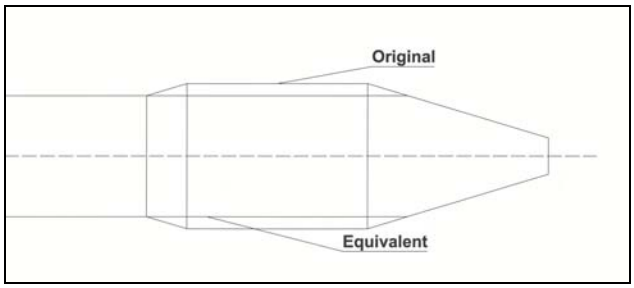

Figure 3- Equivalent payload fairing

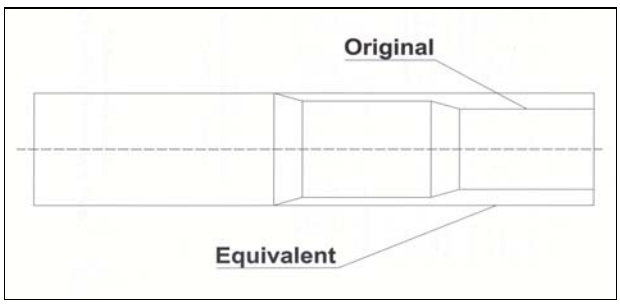

Figure 4- Equivalent core body

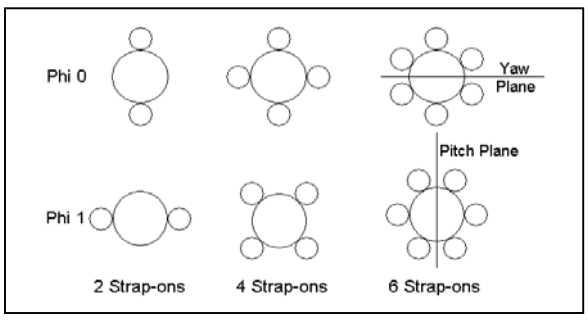

Figure 7- Different ways of positioning strap-ons around the core

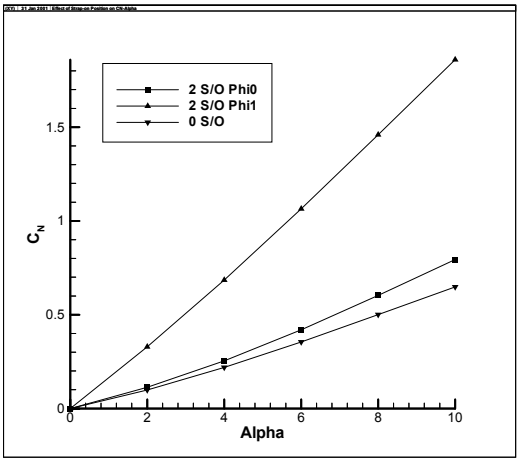

Figure 8- Effect of strap-on position on C_N for 2 strap-ons (M=0.6)

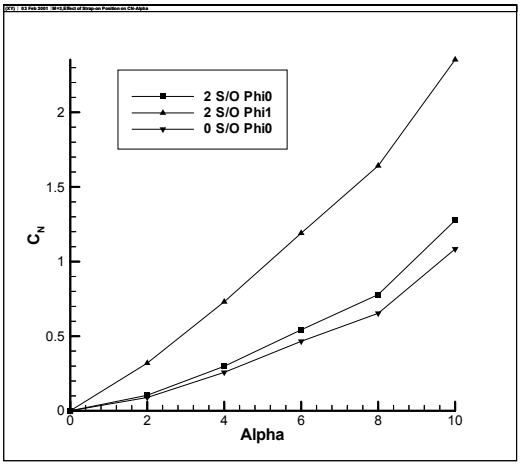

Figure 9- Effect of strap-on position on C_N for 2 strap-ons (M=3.0)

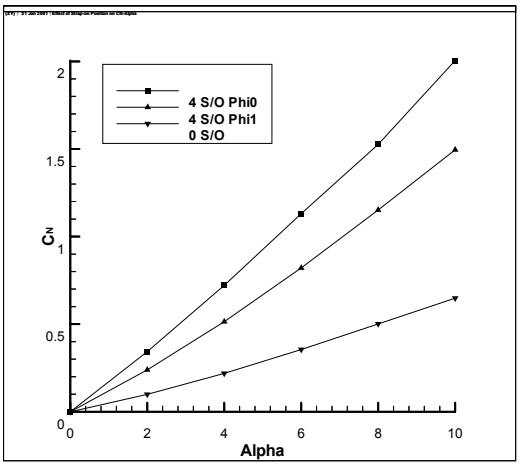

Figure 10- Effect of strap-on position on C_N for 4 strap-ons (M=0.6)

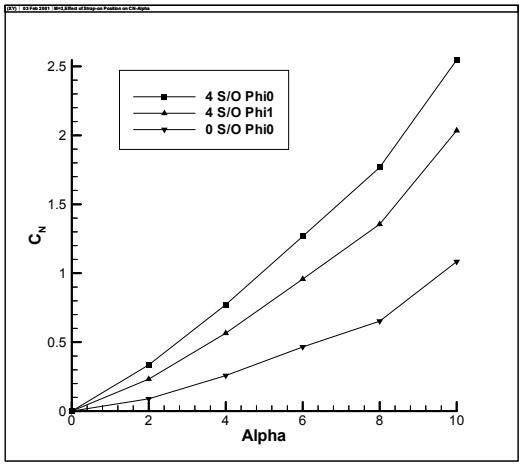

Figure 11- Effect of strap-on position on C_N for 4 strap-ons (M=3.0)

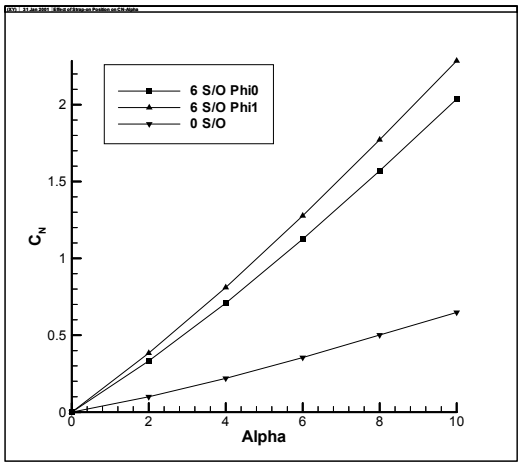

Figure 12- Effect of strap-on position on C_N for 6 strap-ons (M=0.6)

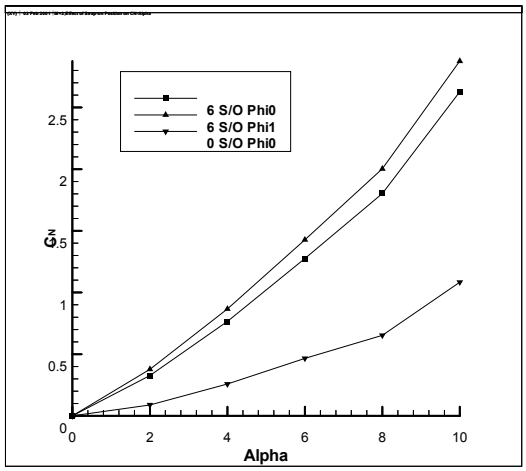

Figure 13- Effect of strap-on position on C_N for 6 strap-ons (M=3.0)

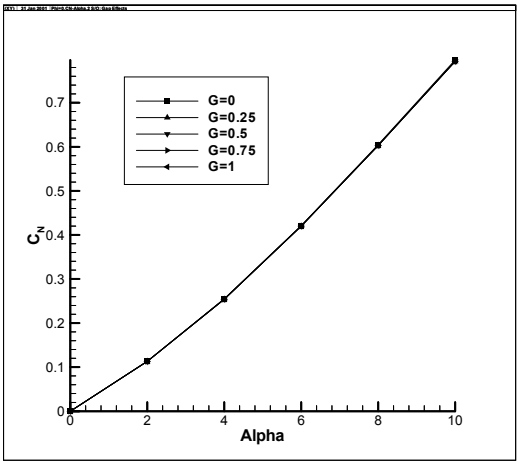

Figure 14- Effect of gap size on C_N (Phi0, M=0.6)

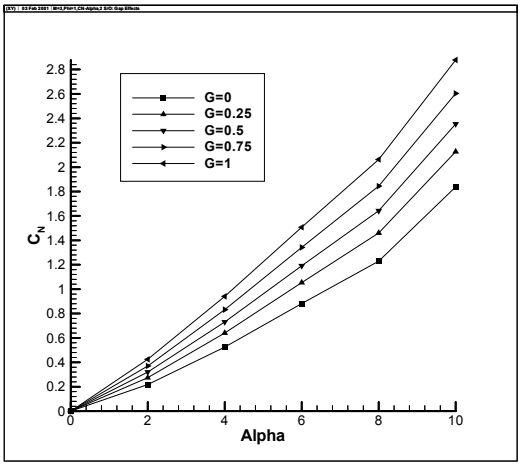

Figure 17- Effect of gap size on C_N (Phi1, M=3.0)

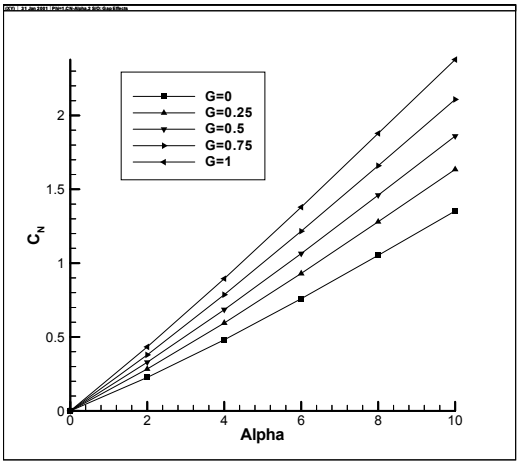

Figure 15- Effect of gap size on C_N (Phi1, M=0.6)

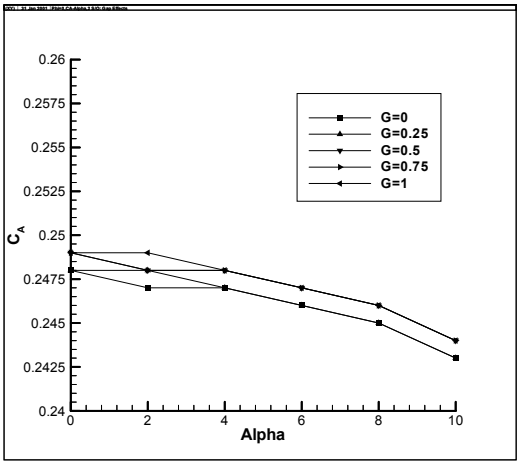

Figure 18- Effect of gap size on C_A (Phi0, M=0.6)

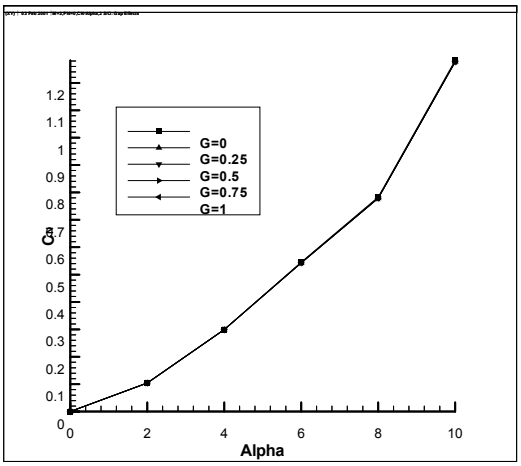

Figure 16- Effect of gap size on C_N (Phi0, M=3.0)

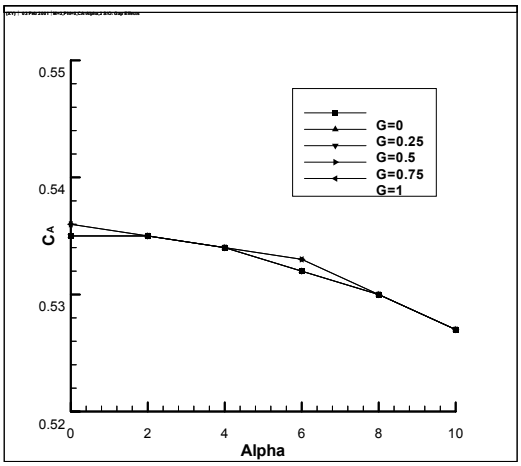

Figure 19- Effect of gap size on C_A (Phi0, M=3.0)

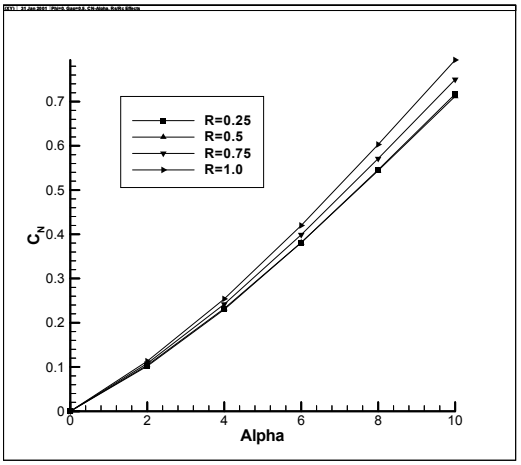

Figure 20- Effect of strap-on radius on C_N (Phi0, M=0.6)

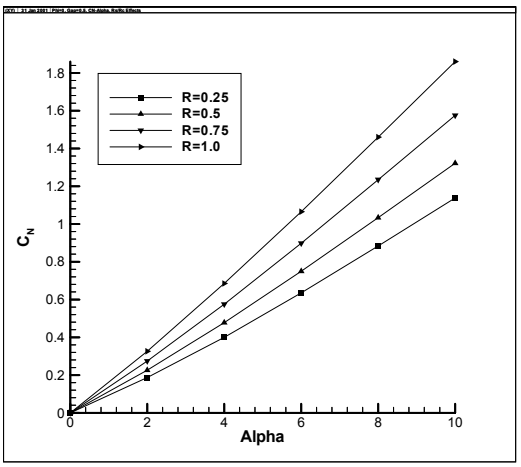

Figure 21- Effect of strap-on radius on C_N (Phi1, M=0.6)

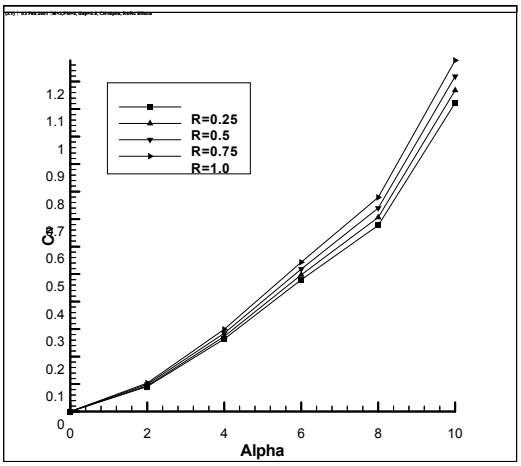

Figure 22- Effect of strap-on radius on C_N (Phi0, M=3.0)

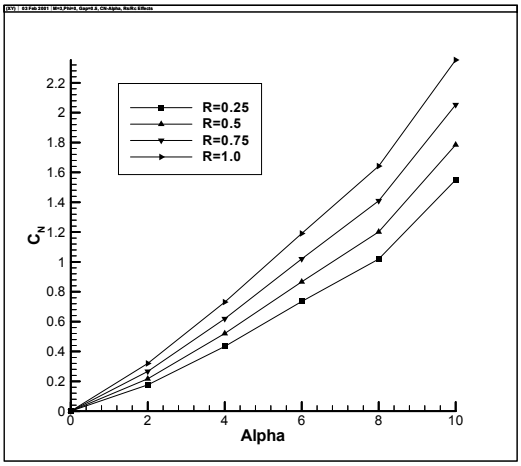

Figure 23- Effect of strap-on radius on C_N (Phi1, M=3.0)

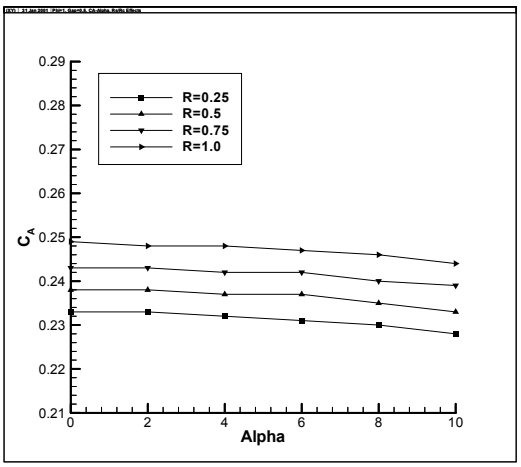

Figure 24- Effect of strap-on radius on C_A (Phi0, M=0.6)

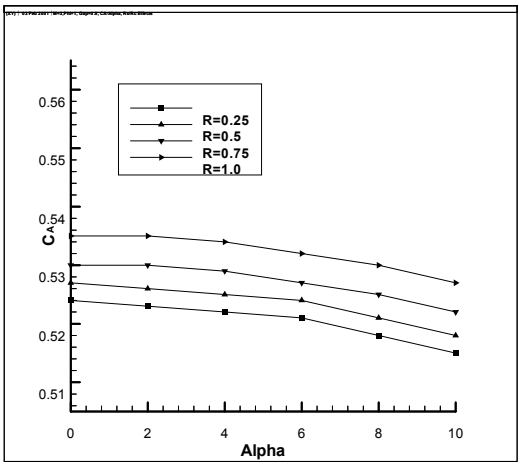

Figure 25- Effect of strap-on radius on C_A (Phi0, M=3.0)

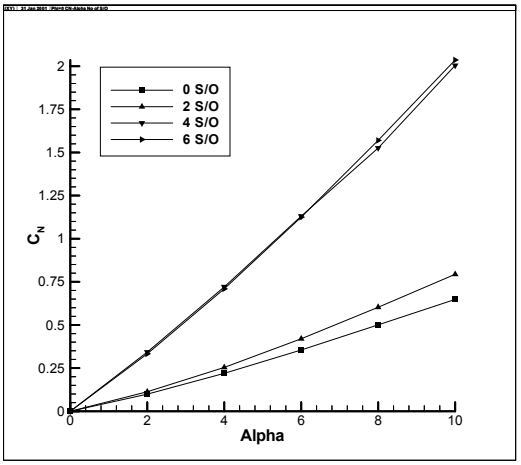

Figure 26- Effect of the number of strap-ons on C_N (Phi0, M=0.6)

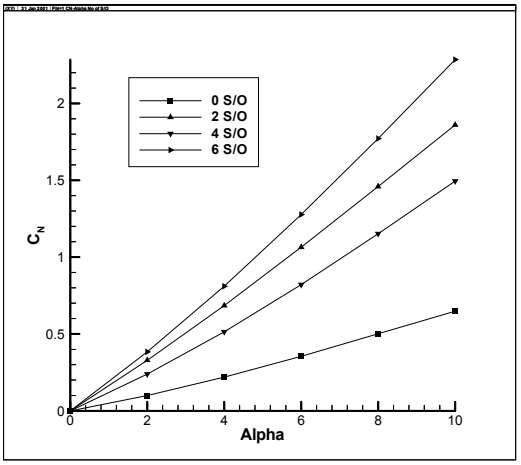

Figure 27- Effect of the number of strap-ons on C_N (Phi1, M=0.6)

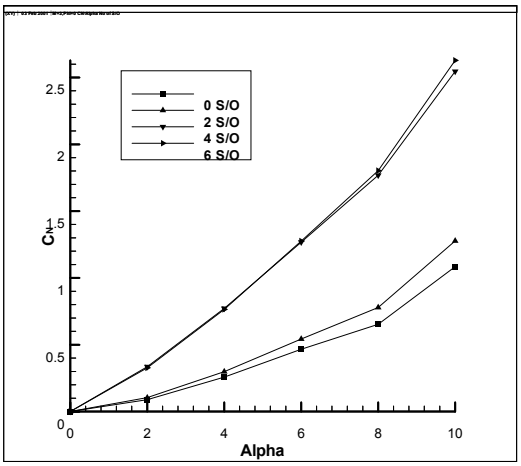

Figure 28- Effect of the number of strap-ons on C_N (Phi0, M=3.0)

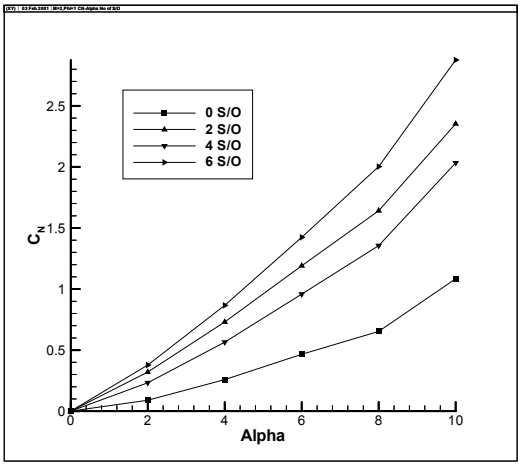

Figure 29- Effect of the number of strap-ons on C_N (Phi1, M=3.0)

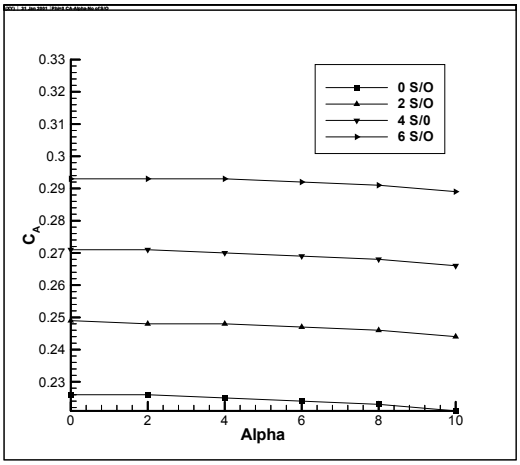

Figure 30- Effect of the number of strap-ons on C_A (Phi0, M=0.6)

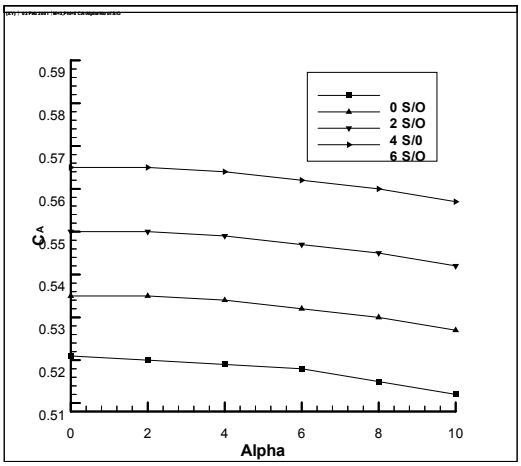

Figure 31- Effect of the number of strap-ons on C_A (Phi0, M=3.0)

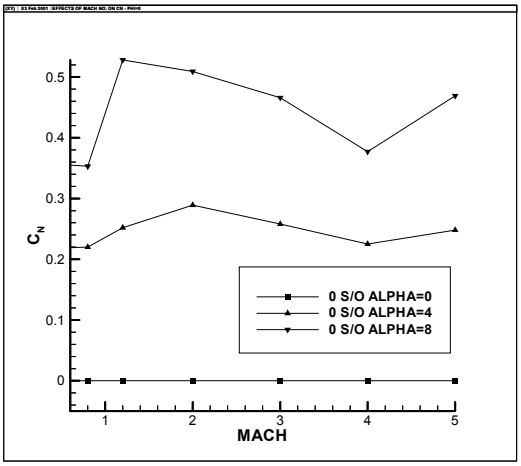

Figure 32- Effect of Mach number on C_N (Body alone)

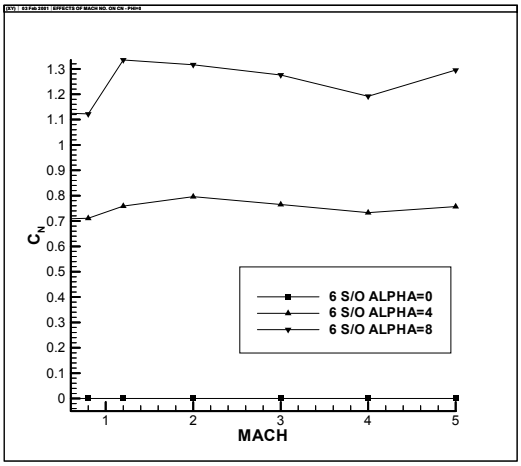

Figure 34- Effect of Mach number on C_N (6 Strap-ons, Phi0)

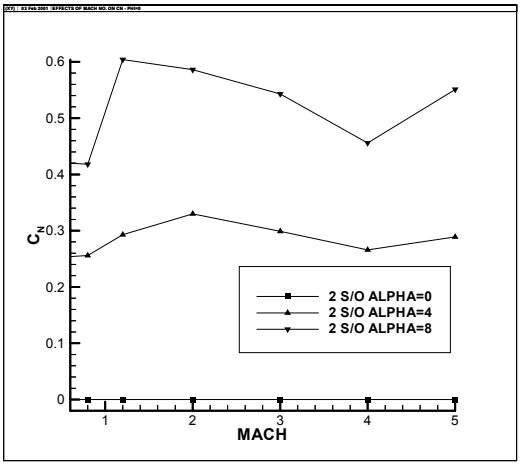

Figure 33- Effect of Mach number on C_N (2 Strap-ons, Phi0)

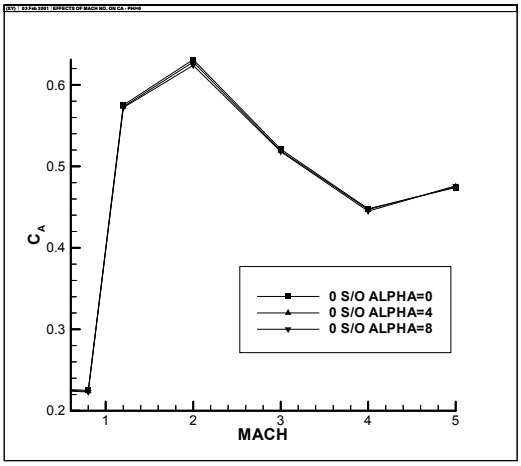

Figure 35- Effect of Mach number on C_A (Body Alone)

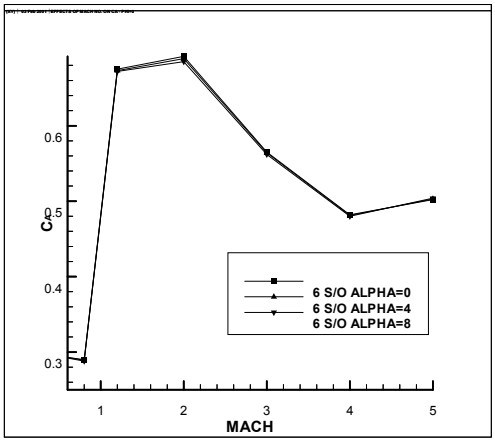

Figure 36- Effect of Mach number on C_A (6 Strap-ons, Phi0)